Arabian Journal of Chemistry (2016) 9, 451–462

King Saud University

Arabian Journal of Chemistry

www.ksu.edu.sa
www.sciencedirect.com

ORIGINAL ARTICLE

Synthesis, photochemical and electrochemical studies on triphenyltin(IV) derivative of (Z)-4-(4-cyanophenylamino)-4-oxobut-2-enoic acid for its binding with DNA: Biological interpretation

Nasima Arshad [a,*], Moazzam H. Bhatti [a], Shahid Iqbal Farooqi [a], Samreen Saleem [b], Bushra Mirza [b]

[a] *Department of Chemistry, Allama Iqbal Open University, Islamabad, Pakistan*
[b] *Department of Biochemistry, Quaid-i-Azam University, Islamabad, Pakistan*

Received 17 July 2013; accepted 13 August 2014
Available online 1 September 2014

KEYWORDS

Triorganotins;
UV–Visible spectroscopy;
Fluorescence spectroscopy;
Cyclic voltammetry;
DNA binding;
Bioactivities

Abstract (*Z*)-4-(4-cyanophenylamino)-4-oxobut-2-enoic acid (LH) and its new triphenyltin (IV) derivative (Ph_3SnL) were synthesized and further investigated for their binding with ds.DNA under physiological conditions {pH: 4.7 (stomach); 7.4 (blood), 37 °C} using UV–Visible/fluorescence spectroscopy, cyclic voltammetry and viscosity measurement techniques. Spectral responses as well as experimental findings from all the techniques i.e., binding constant (K_b), binding site size (n) and free energy change (ΔG) correlated with each other and indicated formation of spontaneous compound–DNA complexes via intercalation of compounds into the DNA base pairs. Values of kinetic parameter, K_b, revealed comparatively greater binding of both the compounds with DNA at stomach pH (4.7). However among both compounds organotin complex (Ph_3SnL) showed comparatively greater binding than that of its ligand (LH) as evident from its, K_b, values at both the pH values. In general, K_b values were evaluated greater for Ph_3SnL at stomach pH {: K_b: $8.65 \times 10^4\ M^{-1}$ (UV); $5.49 \times 10^4\ M^{-1}$ (fluorescence); $8.85 \times 10^4\ M^{-1}$ (CV)}. Voltammetric responses of both compounds before and after the addition of DNA indicated that diffusion controlled processes are involved. Complex Ph_3SnL exhibited the best antitumor activity.

1. Introduction

The increasing interest in organotin(IV) carboxylates in recent years has, to a large extent, been prompted by their structural diversity (Ali et al., 2007; Tiekink, 1991; Tiekink, 1994) and broad therapeutic activity (Hadjikakou and Hahjiliadis, 2009; Nagy et al., 2008). Information on the structural aspects

* Corresponding author. Tel.: +92 51 9057756; fax: +92 51 9250081.
E-mail address: nasimaa2006@yahoo.com (N. Arshad).
Peer review under responsibility of King Saud University.

Production and hosting by Elsevier

http://dx.doi.org/10.1016/j.arabjc.2014.08.018

of organotin(IV) carboxylates is a continuous discussion and at the same time some new applications of high importance are being discovered which are relevant to their medicinal applications (Gielen, 1996; Kaluderovic et al., 2010; Sirajuddin et al., 2014). An immense curiosity in the chemistry of organotin(IV) compounds has led to the extended studies on their reactions with different biomolecules e.g., carbohydrates, nucleic acid derivatives, amino acids and peptides (Yang and Guo, 1999; Nath et al., 2001). In general triorganotin(IV) compounds display a large array of biological activities than their diorganotin and monoorganotin analogues. This has been attributed to their ability to bind with proteins (Pettinari and Marchetti, 2008). Furthermore, many organotin(IV) carboxylates have been found to possess anticancer activity in a variety of tumor cells and the structures of these organotin(IV) compounds have been characterized both in solid and solution forms (Hadjikakou and Hahjiliadis, 2009; El-Sherif, 2012).

In recent years DNA bindings/cleavage with organotin(IV) has become the main subject of study for many researchers (Alama et al., 2009; Camm and McGowan, 2009; Tabassum and Pettinari, 2006; Tabassum et al., 2012; Shujha et al., 2010). Most of the published papers describe experimental and theoretical studies of the interaction of organotin(IV) compounds with DNA. Such organotin(IV)–DNA interactions suggest possible antitumor activities of organotin(IV) compounds. It is well known that DNA itself is an important target of anti-tumor drugs with different types of interactions which can often cause DNA damage in cancer cells, blocking the division of cancer cells and ultimately results in death of cancer cells (Tabassum and Pettinari, 2006). The binding ability of organotin(IV) compounds with DNA depends on the coordination number and nature of the groups bonded to central tin atom. Small molecules bind to DNA through covalent or non-covalent interactions. Such binding can take place either with the nitrogenous bases or negatively charged oxygen of the phosphate backbone of DNA (Tabassum and Pettinari, 2006).

Keeping in view the great importance of organotin carboxylates and in continuation of our previous work on DNA binding studies with different molecules (Arshad et al., 2013; Arshad et al., 2012a,b), present research has been focused on synthesis, characterization and investigation on binding interactions of (*Z*)-4-(4-cyanophenylamino)-4-oxobut-2-enoic acid (LH) and its triphenyltin derivative (Ph_3SnL) with DNA using UV–Visible spectroscopy, fluorescence spectroscopy, cyclic voltammetry, and viscosity measurements. These compounds were also investigated for their antioxidant and antitumor potential by using different bioassays.

2. Materials and methods

2.1. Chemicals and reagents

All reagents were procured from Aldrich/Fluka and used without further purification. All the solvents were dried before use by the literature methods. The ligand (LH) and its triphenyltin(IV) (Ph_3SnL) complex were prepared as given in Schemes 1 and 2. DNA was extracted in the laboratory from chicken blood by the Falcon method (Sambrook et al., 1989) and its concentration was determined spectrophotometrically at 260 nm using molar extinction coefficient, $\varepsilon_{260} = 6600\ cm^{-1}\ M^{-1}$ (Reichmann et al., 1954). Purity of DNA was checked by monitoring the ratio of the absorbance at 260 nm to that at 280 nm and solution gave a ratio of $A_{260}/A_{280} > 1.8$, indicating that DNA was sufficiently pure and free from protein (Babkina and Ulakhovich, 2005). The stock solutions of LH and Ph_3SnL were prepared by dissolving them in buffer solution of pH 4.7 (acetate buffer; $CH_3COOH + CH_3COONa$) and pH 7.4 (phosphate buffer; $Na_2HPO_4 + NaH_2PO_4$). Autoclaved water was used to prepare all the solutions.

2.2. Methods

2.2.1. Synthesis

The ligand precursor (LH) was obtained from the reaction of maleic anhydride with *4*-aminobenzonitrile in ethyl acetate as shown in Scheme 1. A solution of maleic anhydride (0.98 g, 10 mmol) in 50 mL ethyl acetate was added to a solution of *4*-aminobenzonitrile (1.18 g, 10 mmol) in 50 mL ethyl acetate in a 250 mL conical flask. The mixture was stirred for three hours at room temperature. After stirring the precipitates of ligand acid were filtered and recrystallized with ethanol.

The triphenyltin(IV) complex (Ph_3SnL) was obtained from the reaction of Ph_3SnOH with ligand precursor in a 1:1 molar ratio. In a typical procedure, equimolar amounts of ligand precursor (2.16 g, 10 mmol) and triphenyltin hydroxide (3.17 g 10.mmol) were suspended in 100 mL of dry ethanol/acetone (8:2) solvent mixture and refluxed for 8 h. After cooling to room temperature, reaction mixture was filtered and solvents were evaporated in a rotary evaporator. The solid obtained was recrystallized from chloroform with few drops of *n*-hexane. The general chemical reaction is given in Scheme 2.

2.2.2. Physical data

LH: Yield 77%, m.p.: 190–192 °C. FTIR data (KBr, cm^{-1}): ν (NH) 3291, ν (OH) 3204, ν (CN) 2229, ν_{asym} (COO) 1713, ν_{sym} (COO) 1420, $\Delta\nu = 297$, ν (NHCO) 1628.

^{1}H NMR data (DMSO, ppm $^3J(^1H, ^1H)$ in Hz): 12.92 (b, 1H, CONH), 10.73 (s, 1H, H-1), 7.92 (d, 2H, (8.0), H-6,6′), 7.82 (d, 2H, (8.0), H-7,7′), 6.57 (d, 1H, (12), H-2), 6.36 (d, 1H, (12), H-3).

^{13}C NMR data (DMSO, ppm): 166.9 (C1), 130.3 (C2), 131.5 (C3), 163.9 (C4), 142.9 (C5), 119.4 (C6), 118.9 (C7), 133.3 (C8), 105.3 (C9).

Ph_3SnL: Yield 70%, m.p.: 160–162 °C. FTIR data (KBr, cm^{-1}): ν (NH) 3301, ν (CN) 2228, ν_{asym} (COO) 1671, ν_{sym} (COO) 1481, $\Delta\nu = 190$, ν (NHCO) 1622, ν (Sn–O) 454.

^{1}H NMR data ($CDCl_3$, ppm $^3J(^1H, ^1H)$ in Hz): 11.63 (b, 1H, CONH), 7.81 (d, 2H, (8.4), H-6,6′), 7.62 (d, 2H, (8.4), H-7,7′), 7.75–7.68 and 7.54–7.45 (m, 15H, SnPh), 6.38 (d, 1H, (13.2), H-2), 6.28 (d, 1H, (13.2), H-3).

^{13}C NMR data ($CDCl_3$, ppm, $^nJ[^{119}Sn, ^{13}C]$ in Hz): 171.9 (C1), 129.2 (C2), 129.7 (C3), 162.4 (C4), 142.2 (C5), 119.8 (C6), 119.0 (C7), 128.8 (C8), 107.0 (C9), 137.7 [655] (Cα), 136.7 [46.8] (Cβ), 130.7 [22.6] (Cγ), 128.0 (Cδ).

2.3. Instrumentations

The melting points were determined in capillary tubes using a MPD Mitamura Riken Kogyo (Japan) Electro thermal melting point apparatus and were uncorrected. FTIR spectra (KBr) were recorded on a Nicolet iS 10 FTIR spectrophotometer in

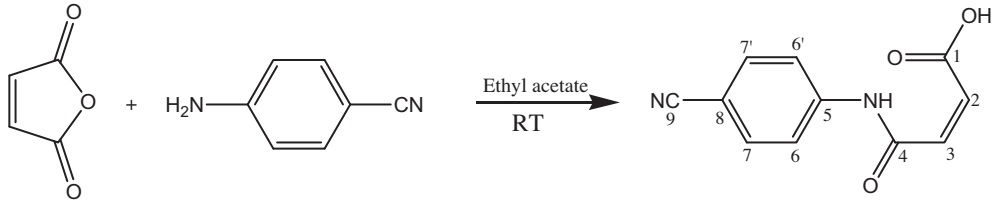

Scheme 1 Synthesis of ligand precursor (LH).

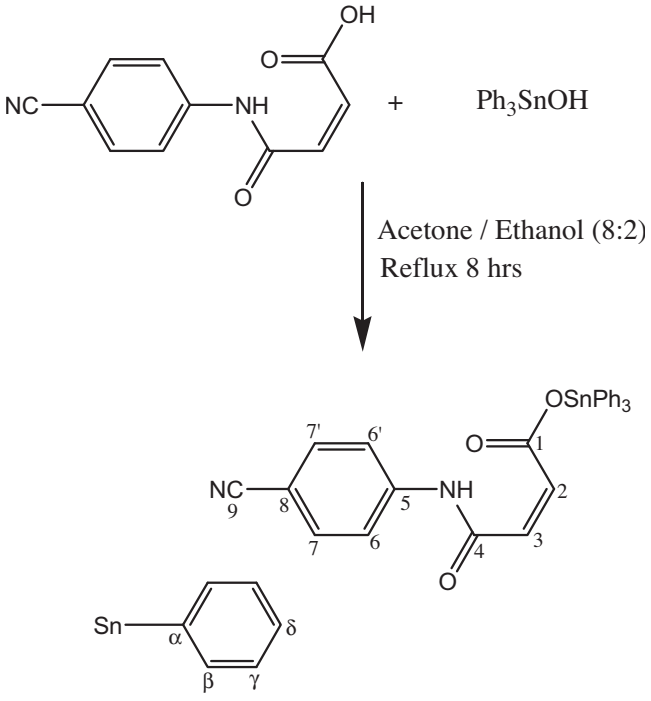

Scheme 2 Synthesis of triphenyltin(IV) complex (Ph_3SnL).

the range of 4000–400 cm^{-1}. The ^{1}H and ^{13}C NMR spectra were recorded on a Bruker Avance 400 spectrometer operating at 400 MHz. The electronic absorption spectra were recorded on a Shimadzu 1800 spectrophotometer (TCC-240A, Japan) equipped with temperature control device using 1.0 cm matched quartz cells. Fluorescent emission spectra were recorded on an F-7000 FL spectrophotometer 2133-007. Cyclic voltammetric experiments were performed using AUTOLAB PGSTAT–302 with GPES version 4.9 (Eco Chemie, Utrecht, Netherlands).

Electrochemical measurements were carried out in a dried conventional three electrode cell using a glassy carbon (GCE; $d = 3$ mm) working electrode, a saturated calomel (SCE; 3.5 M KCl) reference electrode and a Pt sheet counter electrode. Prior to each experiment the GCE was polished with alumina powder and rinsed thoroughly with doubly distilled water and ultrasonicated for 30 s.

2.4. UV–Visible and fluorescence spectroscopy

Concentration of DNA as determined by a UV–Visible spectrophotometer at 260 nm was found 1.8×10^{-4} M. Spectroscopic titrations were carried out at stomach pH (4.7) and blood (7.4) and at 37 °C (body temperature). The absorbance measurements by UV–Visible spectrophotometer and the fluorescence emission spectra by fluorescence spectrophotometer were recorded by keeping the concentration of LH and Ph_3SnL constant (2.8×10^{-5} M) in the sample cell, while varying the concentration of ds.DNA from 10 to 60 μM in the sample cell. In order to achieve the equilibrium between the compound and DNA, solutions were allowed to stay for at least 5 min before each measurement was made. After placing the sample solutions within the cell cavity and before running the spectra, required temperature (37 °C) was maintained on temperature controlled device.

2.5. Cyclic voltammetry

First a blank CV was run with the buffer solutions (4.7 and 7.4) at 37 °C, which showed no electroactivity in the potential range of our interest (−2 to +2 V). Cyclic voltammograms of LH and Ph_3SnL (2.8×10^{-5} M) were recorded from −2.0 to +1.0 V vs. SCE before and after the addition of different volumes (μl) of the stock DNA solution corresponding to the final concentration of DNA ranging from 10 to 60 μM within the cell. Scan rate of 100 mV/s was used throughout the experiments. All measurements were made at 37 °C after purging the solution in the cell with argon gas (99.999%) for at least 10–15 min to exclude oxygen before every electrochemical assay.

2.6. Viscosity measurements

At first viscosity of DNA solution (η_o) was determined at stomach (4.7) and blood (7.4) pH under physiological temperature (37 °C). Then specific viscosity contribution (η), due to DNA (10 μM) in the presence of increasing concentration of investigated compound was determined. The values of the relative specific viscosities for the compounds i.e., $(\eta/\eta_o)^{1/3}$ were then plotted against the ratio; [compound]/[DNA].

2.7. DPPH radical scavenging experiment

DPPH free radical scavenging activity of test compounds was carried out by already reported methods (Arshad et al., 2013; Arshad et al., 2012a; Nawaz et al., 2009). Compounds were examined at four concentrations 7.4, 22.2, 66.6 and 200 μg ml^{-1} as final concentrations from stock. Reaction mixture was prepared by adding 0.1 ml of each test compound solution in DMSO, 2 ml of 0.1 mM DPPH in ethanol solution and 0.9 ml of 50 mM Tris–HCl in capped vials. DMSO was used as negative and ascorbic acid was used as positive control, respectively. Reaction mixture was incubated in the dark for 30 min at room temperature. After incubation, change in

DPPH color was observed by spectrophotometric absorbance at 517 nm. Mixture of all solvents utilized in the assay was used as blank for the spectrophotometer. Percent scavenging of DPPH free radical for each concentration of each compound was calculated.

2.8. Potato disc antitumor assay

Potato disc antitumor assay with some modifications was performed to detect the tumor inhibition activity of compounds under investigation (Arshad et al., 2013; Arshad et al., 2012a; Ahmad et al., 2008). In this assay 48 hour old single colony culture of *Agrobacterium tumefaciens* (At-10) strain was used as tumor inducing agent on potato discs. Each test sample was evaluated for antitumor activity at four concentrations i.e., 7.4, 22.2, 66.6, and 200 μg ml^{-1} with DMSO as negative controls and vincristine as standard drug. Under complete aseptic conditions, potato discs (0.5 cm thickness) were made by using sterilized instruments from surface sterilized ($HgCl_2$ 0.1%) healthy potato tubers. Fifteen potato discs were transferred on each petriplate containing 1.5% agar–agar in distilled water. After treatment with test compounds and At-10 strain on each disc, these petriplates were then incubated at 28 °C for 21 days. Number of tumors was counted after staining with the Lugol's solution (10% KI and 5% I_2) with the help of a dissecting microscope. Percentage tumor inhibition was calculated. Each experiment was carried out in triplicate and IC_{50} values for each compound were calculated.

3. Results and discussion

3.1. Ligand precursor and triphenyltin(IV) complex

The ligand precursor (LH) was obtained from the reaction of maleic anhydride with *4*-aminobenzonitrile in ethyl acetate as shown in Scheme 1 while its triphenyltin(IV) complex (Ph_3SnL) was obtained from the reaction of Ph_3SnOH with ligand precursor in a 1:1 molar ratio as given in Scheme 2. Both ligand precursor and triphenyltin(IV) complex are stable in moist air and soluble in common organic solvents like $CHCl_3$, CH_2Cl_2 and DMSO.

The Infra red spectra of both compounds were recorded in the range of 4000–400 cm^{-1} and important bands are given along with synthesis in experimental section. The tentative assignments are made on the basis of reported literature values and by comparing both compounds. The most significant IR bands are ν(OH), ν(COO) and ν(Sn–O) in both compounds. The explicit feature observed in the spectra of the synthesized triphenyltin(IV) is the absence of the broad band 3204 cm^{-1}, which appears in the free ligand precursor as the ν(O–H) vibration, thus indicating Sn–OCO bond formation through this site. The difference, $[\Delta\nu = \nu_{asym}(COO) - \nu_{sym}(COO)]$, has been used to predict the mode of tin carboxylate interaction and may help to elucidate the structure and bonding mode. The $\Delta\nu$ value of 192 cm^{-1} for the synthesized organotin reflects the bidentate nature of the carboxylic group (Rehman et al., 2012). Thus comparing with earlier report (Bhatti et al., 2013) the tin atom approaches five coordination and carboxylate group acts as bridging bidentate ligand leading to trigonal bipyramidal with trans-R_3SnO_2 geometry. The IR band 454 cm^{-1} indicates the presence of Sn–O bond for the complex.

^1H and ^{13}C NMR for both ligand precursor and organotin complex were recorded in DMSO and $CDCl_3$, respectively and are given along with synthesis in experimental section. The most down field signal in ligand precursor is at 12.92 ppm for the CONH group while acid proton (COOH) appears at 10.73 ppm. Aromatic protons and ethylene protons appear as doublet in the expected range. The disappearance of signal of acid proton in the spectrum of Ph_3SnL further strengthens the formation of complex. In addition, the phenyl group attached with Sn atom gives complex multiplets in range of 7.45–7.75 ppm. In ^{13}C NMR the carboxylate carbon resonates organotin complex at 171.9 ppm while this carboxylate carbon appears at 166.9 ppm in ligand precursor, reflecting the participation of the COO group in coordination with tin. Tin-phenyl carbons resonate in expected range with well defined tin-carbon $^nJ[^{119}Sn–^{13}C]$ couplings. In mass spectrum of ligand precursor, molecular ion peak $[M^{+\cdot}]$ appears at 216 (10) while low intensity molecular ion peak $[M^{+\cdot}]$ is observed at 566 (3) in case of organotin complex.

3.2. DNA binding study by UV-spectroscopy

UV–Visible spectral changes before and after the addition of various concentrations of compound into the fixed concentration of DNA lead to predict interaction and binding mechanism of compound with DNA (Ruiz et al., 2011).

In present studies, pure spectra of LH and Ph_3SnL both having same concentration (2.8×10^{-5} M) were recorded separately, Fig. S1 (in supplementary information). All solutions were prepared in ethanol-water mixture (7:3). A single peak for LH and Ph_3SnL compounds appears at λ_{max} of 288.2 and 302 nm respectively. The molar extinction coefficient (ε) values were evaluated as 16,025 cm^{-1} M^{-1} and 14,612 cm^{-1} M^{-1} respectively for LH and Ph_3SnL and indicated that π-π^* transitions are operative for both compounds in the λ_{max} range of 240–390 nm, Figs. S2 and S3 (concentration profile; in supplementary information). Absorption spectrum of pure chicken blood ds-DNA recorded in double deionized distilled water showed a broad band at λ_{max} of 260 nm. The observed maximum arises due to purine and pyrimidine moieties having chromophoric centers. The absorbance ratio (A_{260}/A_{280}) assured that DNA is pure as its value was found to be 1.83 (Babkina and Ulakhovich, 2005).

After the addition of varying concentrations of DNA (10–60 μM) on a fixed concentration (2.8×10^{-5} M) of LH and Ph_3SnL, hypochromic effect (a gradual decrease in absorbance peak intensity) of extent 46.34% and 49.89% respectively at pH 4.7 and 44.46% and 47.76% respectively at pH 7.4 along with gradual blue shift of magnitude 6.4 and 8.6 nm respectively at pH 4.7 and 2.0 and 4.0 nm respectively at pH 7.4 was observed in the UV-spectra, Fig. 1. Percent decrease in the absorption peak intensities of LH and Ph_3SnL in the presence of DNA was calculated, using Eq. (1).

$$H\% = \frac{A_{free} - A_{bound}}{A_{free}} \times 100 \quad (1)$$

Change in the spectral behavior of both the compounds after the addition of DNA inferred their binding with the DNA (Tabassum et al., 2012; Arshad et al., 2013; Arshad et al., 2012a; Ruiz et al., 2011). Further, hypochromic effect after the addition of DNA is evocative of compound–DNA complex

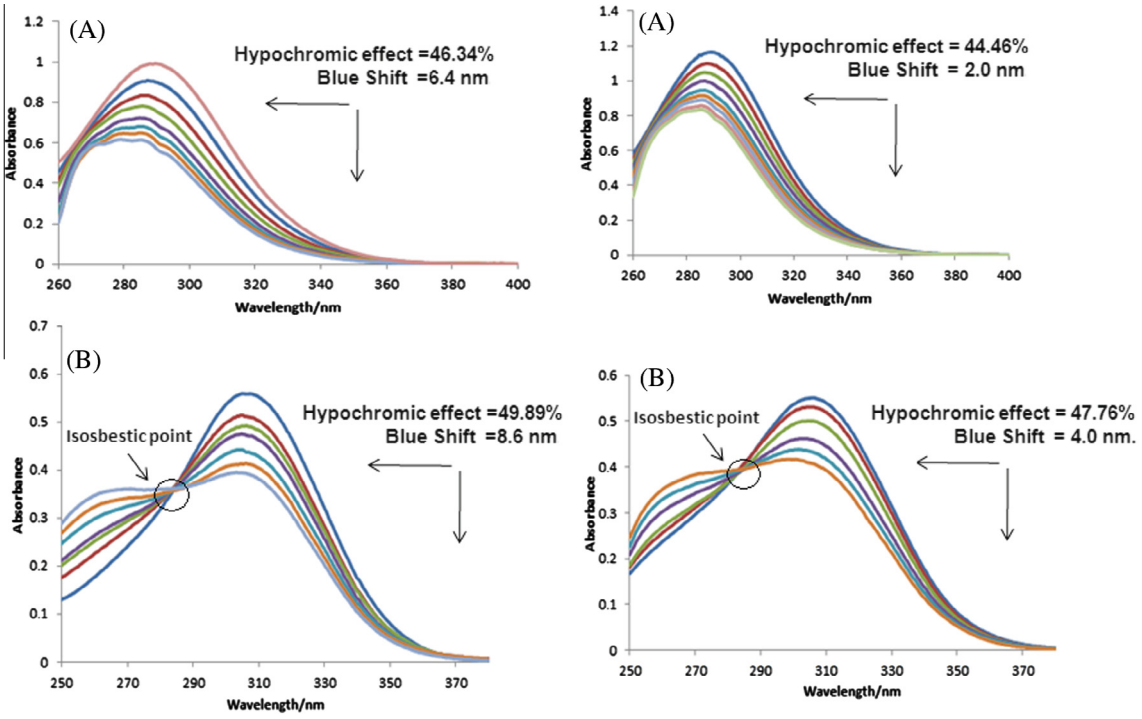

Figure 1 UV-spectra for (A) LH, (B) Ph_3SnL, (2.8×10^{-5} M) without and in the presence of 10–60 μM DNA at pH 4.7 (left hand side) and pH 7.4 (right hand side) and at 37 °C. The arrow direction indicates increasing concentrations of DNA.

formation via intercalation. Intercalation of a compound into the DNA base pairs generally arises due to the overlapping of π^*-orbital of intercalated ligand with π-orbital of the base pairs. Transition probabilities decrease due to partially filled coupling π-orbital of DNA and as a consequence hypochromism is observed in the spectra (Xu et al., 2008).

Furthermore, spectra of Ph_3SnL–DNA complex were followed by an isosbestic point at both the pH values, Fig. 1, which is indicative of an equilibrium between bound DNA and the free form of the compounds and that no species other than the free and the intercalated complexes is present in the reaction mixture (Kohn et al., 1975).

Variation in the absorbance spectrum of a compound after the addition of DNA leads to determine the binding kinetics i.e., binding/formation constant "K_b" of compound–DNA complex with the help of Benesi-Hildebrand equation (Kuntz et al., 1968). Using UV-absorption data in Hildebrand equation, K_b values for LH and Ph_3SnL for their binding with DNA were evaluated at both stomach (4.7) and blood (7.4) pH and at temperature 37 °C.

$$\frac{A_o}{A - A_o} = \frac{\varepsilon_G}{\varepsilon_{H-G} - \varepsilon_G} + \frac{\varepsilon_G}{\varepsilon_{H-G} - \varepsilon_G} \frac{1}{K_b[\mathrm{DNA}]} \quad (2)$$

where A_o and A are the absorbance, while E_G and E_{H-G} are the molar extinction coefficient of compound and complex respectively. From the plot of $A_o/(A - A_o)$ to 1/[DNA], the ratio of the intercept to the slope gave the values of binding constant, K_b, Fig. 2, Table 1.

The order of magnitude of binding constant at both the pH values (10^4 M^{-1}) for both investigated compounds revealed their stronger binding with DNA via intercalation. K_b values calculated for both compounds–DNA complexes at both the pH values were found comparatively greater than that of a typical intercalator lumazine–DNA complex whose value was reported as 1.74×10^4 M^{-1} in phosphate buffer of pH (7.2) (Ibrahim et al., 2002). Similarly the binding values of both

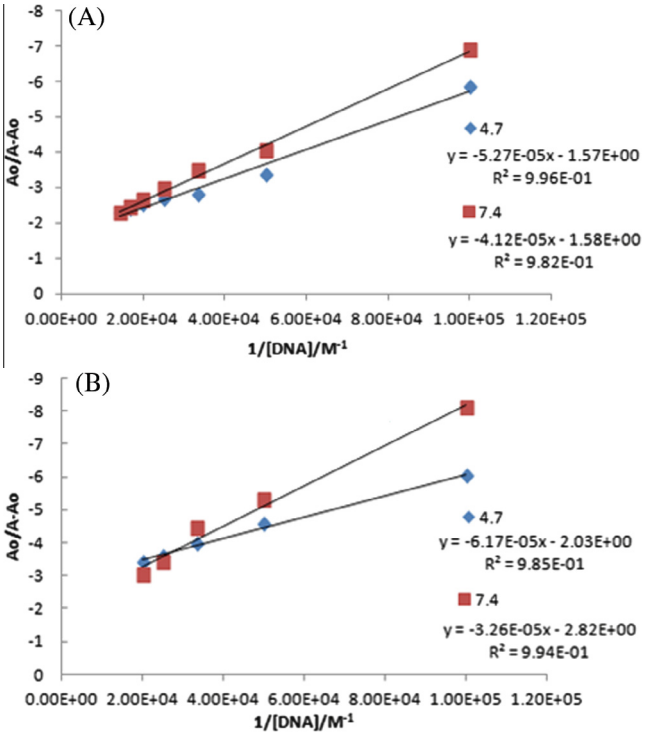

Figure 2 Plots of $A_o/A - A_o$ vs. 1/[DNA] for the application of Benesi-Hildebrand equation for calculation of (A) LH–DNA, (B) Ph_3SnL–DNA binding constant at pH 4.7 and 7.4 and at 37 °C.

Table 1 Binding constants and free energy values for the compounds–DNA complexes from UV-spectrophotometric data at pH 4.7 and 7.4 and at body temperature (37 °C).

Complex code	pH 4.7		pH 7.4	
	Binding constant K_b/M^{-1}	Free energy $(-\Delta G)$ kJ mol^{-1}	Binding constant K_b/M^{-1}	Free energy $(-\Delta G)$ kJ mol^{-1}
LH–DNA	3.83×10^4	27.20	2.97×10^4	26.54
Ph_3SnL–DNA	8.65×10^4	29.30	3.04×10^4	26.60

Table 2 Binding constants and free energy values for the compounds–DNA complexes from fluorescence spectroscopic data at pH 4.7 and 7.4 and at body temperature (37 °C).

Complex code	pH 4.7			pH 7.4		
	Binding constant K_b/M^{-1}	Binding site size (n)	Free Energy $(-\Delta G)$ kJ mol^{-1}	Binding constant K_b/M^{-1}	Binding site size (n)	Free Energy $(-\Delta G)$ kJ mol^{-1}
LH–DNA	2.51×10^4	1.04	25.106	2.40×10^4	1.03	24.695
Ph_3SnL–DNA	5.49×10^4	1.12	27.179	2.77×10^4	1.05	26.645

Table 3 Diffusion coefficients of LH and Ph_3SnL before and after the addition of DNA at pH 4.7 and 7.4 and at body temperature (37 °C).

Compound	D_o ($cm^2\ s^{-1}$) at pH 4.7		D_o ($cm^2\ s^{-1}$) at pH 4.7	
	Before the addition of DNA	After the addition of DNA	Before the addition of DNA	After the addition of DNA
LH	9.98×10^{-10}	6.69×10^{-12}	9.84×10^{-10}	7.43×10^{-12}
Ph_3SnL	1.30×10^{-10}	2.21×10^{-11}	2.73×10^{-10}	3.34×10^{-11}

compounds–DNA complexes were found greater than that of another important intercalator proflavine ($K = 2.32 \pm 0.41 \times 10^4\ M^{-1}$) and a clinically used chemotherapeutic agent epirubicin ($K = 3.4 \times 10^4\ M^{-1}$) (Aslanoglu, 2006; Charak et al., 2011), specially at stomach pH (4.7) and are also in good agreement with that reported for anthracycline molecules for their binding with DNA ($K \approx 10^4$–$10^5\ M^{-1}$) (Li et al., 2005). This comparison showed stronger interactions of both the compounds with DNA and their importance as prior competitor in the queue of potential anticancer drug candidates. Binding constants at stomach pH (4.7) for both compounds were evaluated comparatively greater than that at pH (7.4), Table 1. In addition, greater K_b values at stomach pH (4.7) are presumed to the formation of comparatively more stable complex formation of the compounds with DNA at this pH than that at blood pH (7.4), (Arshad et al., 2012a,b), Table 1. The greater binding constants of investigated compounds at both the pH values may further be attributed to their structural planarity due to phenyl groups in the investigated compounds (Arshad et al., 2013; Arshad et al., 2012a). Binding order of both the compounds at pH 4.7 and pH 7.4 is given below.

$K_b(Ph_3SnL) > K_b(LH)$

(At both stomach 4.7 and blood 7.4pH)

and

$K_b(\text{stomach;4.7 pH}) > K_b(\text{blood;7.4 pH})$

Gibbs free energy changes ΔG of compounds–DNA complexes were calculated using Eq. (3). The values were found negative which indicated the involvement of spontaneous processes during compounds–DNA complex formation (Ibrahim et al., 2002), Table 3.

$$\Delta G = -RT \ln K_b (\text{kJ mol}^{-1}) \quad (3)$$

The sequence in ΔG values of the compounds–DNA complexes was found same as for binding constant values at both stomach and blood pH i.e. ΔG (Ph_3SnL) > ΔG (LH), at both stomach 4.7 and blood 7.4 pH and ΔG (stomach; 4.7 pH) > ΔG (blood; 7.4 pH).

3.3. DNA binding study by fluorescence-spectroscopy

Compound–DNA binding interaction could be probed through fluorescence-spectroscopy by direct addition of different concentrations of DNA, bearing in mind that the investigated compound is fluorescence active (Arjmand et al., 2012). The intrinsic fluorescence emission spectra of LH and Ph_3SnL were recorded separately and both compounds were found luminescent, Fig. S4 (in supplementary information).

Then spectral responses of both compounds were recorded separately by gradually adding concentrations of DNA from 10 to 60 μM. The effect on the fluorescence emission spectra of compounds LH and Ph_3SnL is given in Fig. 3. Upon addition of DNA, enhancement in the emission intensities of LH and Ph_3SnL was recorded to be greater than those in the absence of DNA as 3.26 and 4.25 times respectively at pH 4.7 and 3.12 and 4.05 times respectively at pH 7.4. This increase in the emission intensity after the addition of DNA is indicative of compound–DNA complex formation via intercalative mode of interaction (Arjmand et al., 2012).

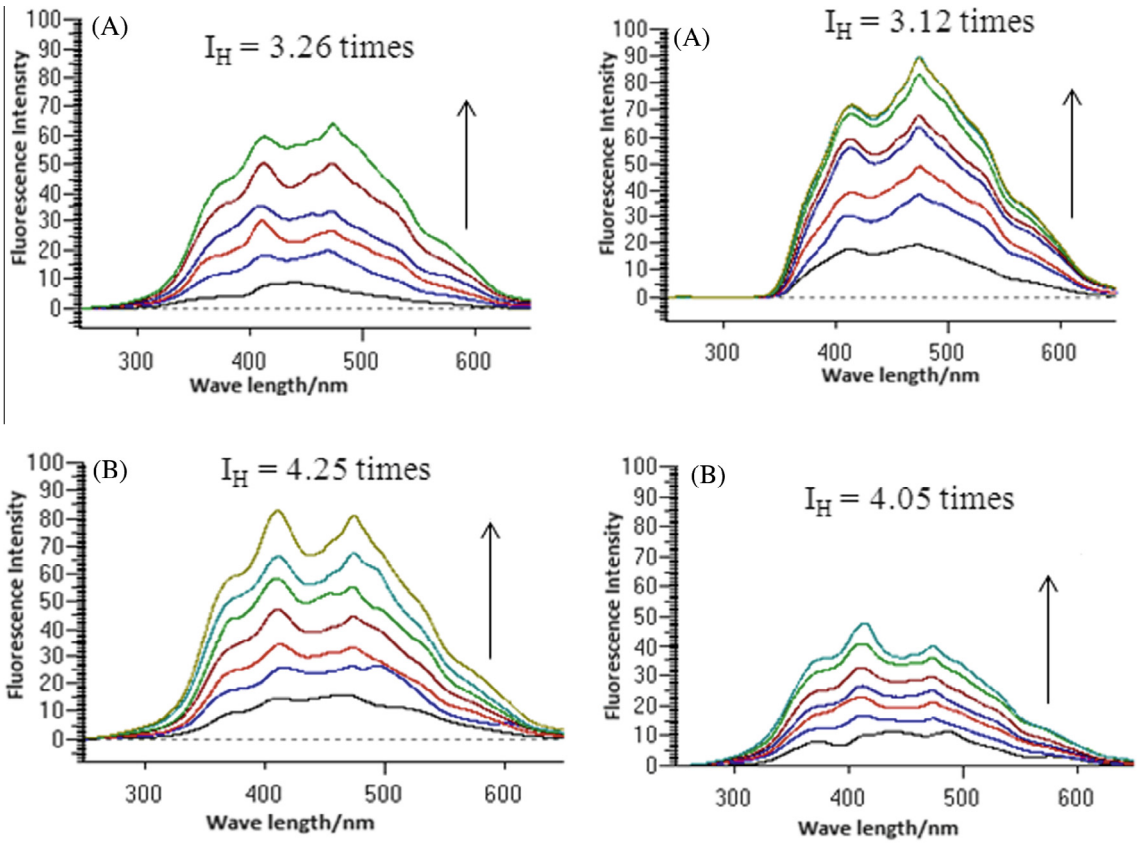

Figure 3 Fluorescence emission spectra for (A) LH and (B) Ph_3SnL (2.8×10^{-5} M) without and in the presence of 10–60 μM DNA at pH 4.7 (left hand side) and pH 7.4 (right hand side) and at 37 °C. The arrow direction indicates increasing concentrations of DNA.

Enhancement in the fluorescence emission intensity of the interacting compound due to its hydrophobic intercalation into the stacked bases of DNA is indicative of the rise in its quantum efficiency and that the compound is protected from the water molecules by the hydrophobic microenvironment of nitrogenous bases inside the DNA-helix (Ruiz et al., 2011). As a result mobility of the compound is restricted at the binding sites which then reduce the vibrational mode of relaxation after excitation and a visible increase is observed in fluorescence emission intensity during compound–DNA complex formation (Feng et al., 1998).

Since fluorescence emission intensity is varied after addition of DNA, the binding constant "K_b" of pro-drug–DNA complex can be determined from the variation in fluorescence emission intensity spectra. Binding constant "K_b" and binding stoichiometry have been evaluated spectrophotometrically by using the following equation (Shahabadi and Fatahi, 2010).

$$\log \frac{F - F_o}{F} = \log K_b + n \log[\text{DNA}] \quad (4)$$

where, F_o and F are the fluorescence intensities of the fluorophore in the absence and in the presence of different concentrations of DNA, respectively. K_b and n are the binding constant and binding site size (binding stoichiometry) respectively which were determined by plotting log $[(F - F_o)/F]$ vs. log [DNA], Fig. 4 (only shown for Ph_3SnL–DNA at both pH values and at 37 °C, for LH–DNA provided as Fig. S5 in supplementary information).

Binding constant, binding site size (n) values of both the compounds were calculated and given in Table 2. The data obtained for K_b from fluorescence spectroscopy are compatible with those obtained from UV-results and further verified stronger binding of compounds with DNA via intercalation at both pH values and the formation of most stable complexes of Ph_3SnL and LH with DNA at stomach pH. The binding site sizes (n) evaluated for both compound–DNA complexes were found to be slightly greater than 1 ($n > 1$) at both pH values, Table 2. It showed that both compounds might have binding with DNA double helix through hydrogen bonding along with the intercalative binding of planar phenyl groups present in investigated compounds (Arshad et al., 2013; Arshad et al., 2012a; Xu et al., 2005). The negative values of ΔG calculated through fluorescence results further supported the UV-results of free energy changes and indicated the spontaneous binding of both the compounds with DNA, Table 2. The orders of K_b and ΔG values of the compounds–DNA complexes at both pH values were found similar as obtained by UV-spectroscopy.

3.4. DNA binding study by cyclic voltammetry

Cyclic voltammetry is considered one of the well-liked techniques for the study of DNA binding with small molecule depending on the fact that compounds bound to DNA are redox active (Hajin et al., 2012). Electrochemical behavior of compounds LH and Ph_3SnL was investigated using the cyclic voltammetric technique in ethanol–water mixture (7:3) at a

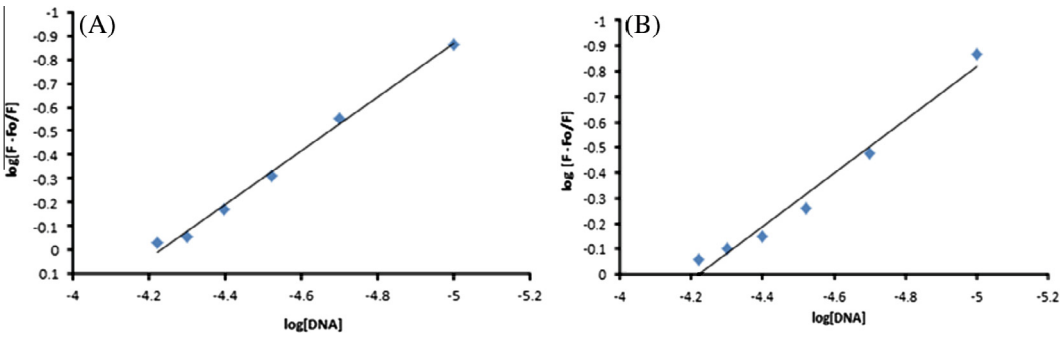

Figure 4 Plots of log $[(F - F_o)/F]$ vs. log [DNA] for the calculation of Ph_3SnL–DNA binding constant and binding site size at pH 4.7 (A) and 7.4 (B) and at 37 °C.

scan rate of 100 mV/s and at glassy carbon electrode surface. LH and Ph_3SnL showed irreversible reduction processes and a single peak was observed at reduction potential (E_{Pc}) of −0.896 V, −0.915 V, respectively at pH 4.7 and −0.878 V, −0.865 V, respectively at pH 7.4 (Fig. S6 in supplementary information). Peak broadening was observed for all the compounds at both pH values, which may be attributed to one step two electron reduction process (Shujha et al., 2010).

Voltammetric responses were recorded after the addition of 1–60 μM DNA on optimized concentration (2.8×10^{-5} M) of LH and Ph_3SnL at both pH values. A decrease in peak height {(LH; 48.8% (pH 4.7), 47.2% (pH 7.4) and Ph_3SnL; 64.4% (pH 4.7), 62.3% (pH 7.4)} was observed along with a negative shift in the reduction peak potential {(LH; 18 mV (pH 4.7), 29 mV (pH 7.4) and Ph_3SnL; 53 mV (pH 4.7), 46 mV (pH 7.4)}, Fig. 5. Such changes in the cyclic voltammogram of a redox active compound after the addition of DNA have been reported for compound–DNA complex formation via intercalation (Arshad et al., 2013; Arshad et al., 2012b; Niranjana et al., 2008).

Randles-Sevcik equation is used to determine the diffusion coefficient values of LH and Ph_3SnL without and in the presence of DNA (Randles, 1948; Sevcik, 1948).

$$I_p = 2.99^5 n(\alpha n_\alpha)^{1/2} A C_o^* D_o^{1/2} v^{1/2} \quad (5)$$

where, I_p is peak current in amperes (A), n is charge transfer number, $n\alpha$ is number of electrons transferred up to and including the rate determining step, α is transfer coefficient (generally, $0.3 < \alpha < 0.7$), A is surface area of the electrode (cm^2), C_o^* is bulk concentration of the electro active species

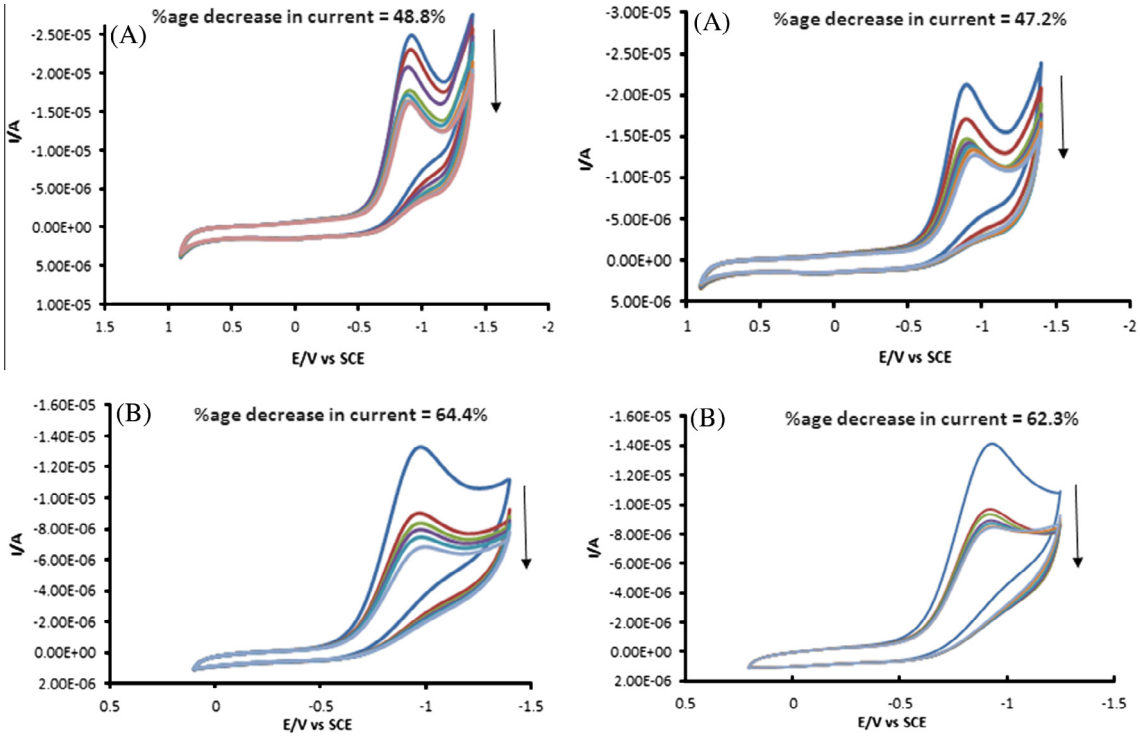

Figure 5 Cyclic voltammetric responses for (A) LH and (B) Ph_3SnL (2.8×10^{-5} M) without and in the presence of 10–60 μM DNA at pH 4.7 (left hand side) and pH 7.4 (right hand side) and at 37 °C. The arrow direction indicates increasing concentrations of DNA.

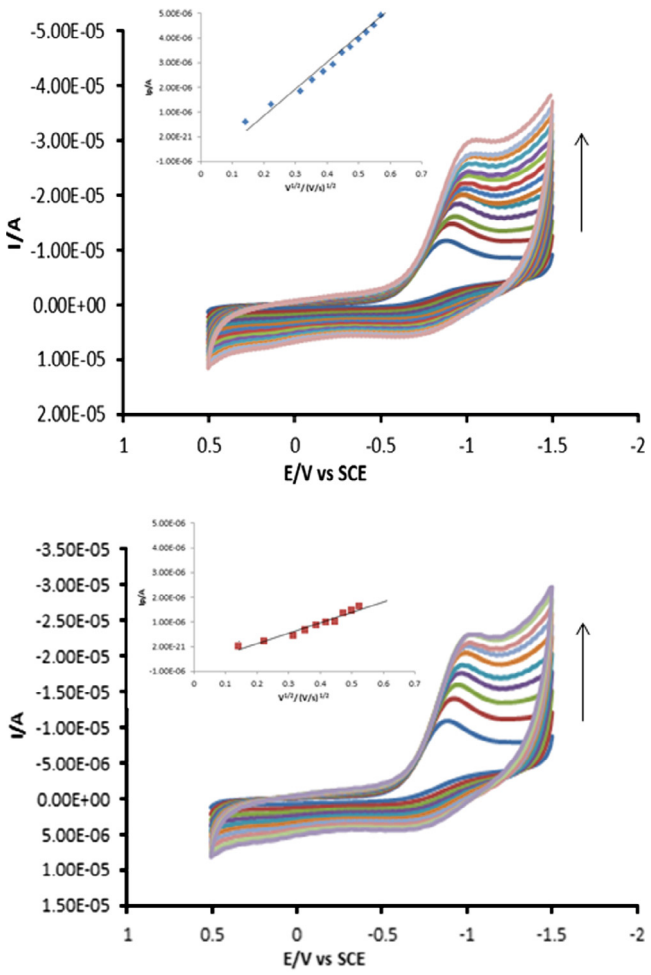

Figure 6 Cyclic voltammogram for Ph_3SnL at different scan rates (Vs^{-1}) in ethanol-water mixture (7:3) in the absence (top) and in the presence (bottom) of ds-DNA at pH 4.7. The arrows direction indicates increasing scan rates (Vs^{-1}) as; 0.02, 0.05, 0.075, 0.1, 0.125, 0.15, 0.175, 0.2, 0.225, 0.25, 0.275, 0.30, 0.325, and 0.350. Inset: Plots of I_p vs. $v^{1/2}$ for Ph_3SnL (2.8×10^{-5} M) at pH 4.7 (acetate buffer) in the absence (top) and in the presence of 60 μM DNA (bottom) at various scan rates (Vs^{-1}).

(mol cm^{-3}), v is potential scan rate in Vs^{-1} and D_o is diffusion coefficient ($cm^2\ s^{-1}$).

I_p values were plotted vs. $v^{1/2}$ for both compounds without and in the presence of DNA which showed linear dependency of peak currents on the square root of scan rates, Fig. 6 (only shown Ph_3SnL at pH 4.7 (others provided as Fig. S7 in supplementary information)). The linearity of plots verified that main mass transport of these electro active species and their DNA bound complexes is diffusion controlled (Arshad et al., 2012b). A negative shift in the peak potential along with an increase in peak current by increasing the scan rate may further be attributed to irreversible nature of redox process (Niranjana et al., 2008) occurring in compounds with and without the addition of DNA, Fig. 6. Number of electrons (n) were calculated using equation; $E_p - E_{p/2} = 47.7\ \text{mV}/\alpha n$. Assuming the value of α to be 0.5, the values of n for both compounds were evaluated approximately equal to 2 which suggests that redox reaction of compounds is an irreversible process and two electrons are involved in the one step reduction process (Wang et al., 2011).

The diffusion coefficients of compounds LH and Ph_3SnL before and after the addition of DNA were calculated and given in Table 3. The lower diffusion coefficient (D_o) values of DNA bound organotin carboxylates are responsible for the decay of peak current in cyclic voltammograms, Fig. 6.

The binding constants, K_b, for both the compounds for their complexation with DNA were calculated according to the following equation which is based on variation in peak currents as in present studies decrease in peak current of compounds by the addition of different concentrations of DNA was observed, (Niu et al., 1994).

$$I_p^2 = \frac{1}{K_b[\text{DNA}]}\left(I_{po}^2 - I_p^2\right) + I_{po}^2 - [\text{DNA}] \tag{6}$$

where K_b is the binding constant, I_p and I_{po} are the peak currents with and without DNA. A plot of I_p^2 vs. $(I_{po}^2 - I_p^2)/[\text{DNA}]$ gave a straight line with a slope equal to the reciprocal of binding constant, K_b, Fig. 7 (only shown for Ph_3SnL–DNA at both pH values and at 37 °C, for LH–DNA provided as Fig. S8 in supplementary information).

The binding constant values were calculated and given in Table 4. Both the compounds showed stronger binding with DNA at stomach pH as evident from comparatively greater K_b values at this pH, Table 4. K_b values obtained through voltammetric parameters were also found in good agreement with those obtained from UV- and fluorescence results hence confirming the compatibility of binding constant results from all the three complementary techniques. Gibbs free energy changes evaluated through K_b data using CV parameters were found as negative values as obtained through UV- and fluorescence results and further inveterate the involvement of

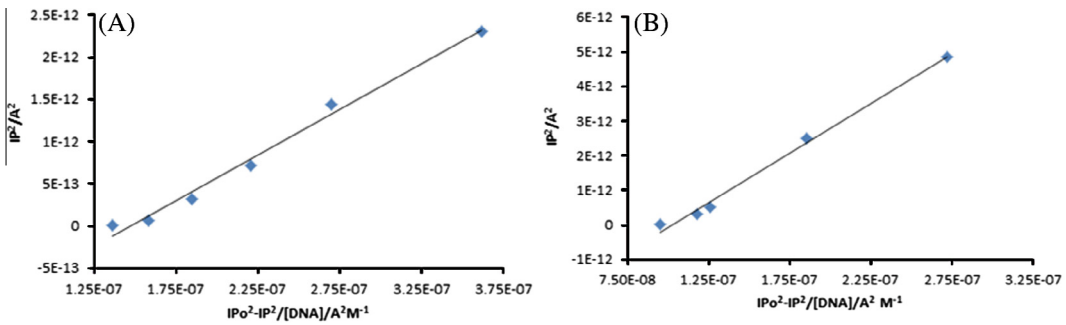

Figure 7 Plots of I_p^2 vs. $I_{po}^2 - I_p^2/[\text{DNA}]$ for calculation of binding constant of Ph_3SnL–DNA adducts at pH 4.7 (A) and 7.4 (B) and at 37 °C.

Table 4 Binding constants and free energy values for the compounds–DNA complexes from voltammetric data at pH 4.7 and 7.4 and at body temperature (37 °C).

Complex code	pH 4.7			pH 7.4		
	Binding constant K_b/ M^{-1}	Binding site size (n)	Free Energy ($-\Delta G$) kJmol^{-1}	Binding constant K_b/ M^{-1}	Binding site size (n)	Free Energy ($-\Delta G$) kJmol^{-1}
LH–DNA	5.35×10^4	1.34	28.1	2.6×10^4	1.05	26.2
Ph_3SnL–DNA	8.85×10^4	2.84	29.4	3.58×10^4	2.07	36.9

Table 5 Antitumor activity of the compounds as evaluated by potato disc antitumor assay and their IC_{50} values.

Sample code	IC_{50} (μg ml^{-1})
LH	149.77
Ph_3SnL	14.02
Vincristine	0.003
DMSO	–

spontaneous process in compound–DNA binding, Table 5. The orders in the value of binding constant as well as free energy change were found to be identical as obtained by both spectroscopic techniques at both pH values.

Kinetics and thermodynamic studies through all the complementary techniques revealed that both LH and Ph_3SnL compounds bind comparatively more strongly and more spontaneously with ds.DNA at stomach pH (4.7) than that at blood pH (7.4). Also, among both the compounds tin complex (Ph_3SnL) showed comparatively greater binding than that of its ligand (LH) at both the pH values.

Binding site sizes (n) were evaluated through cyclic voltammetry by using the following equation (Carter et al., 1989).

$$C_b/C_f = K[\text{free base pairs}]/s \quad (7)$$

where, s is the binding site size in terms of base pairs (bp). Measuring the concentration of DNA in terms of compound concentration, the concentration of the base pairs can be expressed as [DNA]/2. So Eq. (7) can be written as:

$$C_b/C_f = K[\text{DNA}]/2\,s \quad (8)$$

C_f and C_b denote the concentration of the free and DNA bound species respectively. The C_b/C_f ratio was determined by the equation given below (Aslanoglu et al., 2000).

$$C_b/C_f = I - I_{\text{DNA}}/I_{\text{DNA}} \quad (9)$$

where I and I_{DNA} represent the peak currents of the compound in the absence and in the presence of DNA, respectively. Putting the value of K_b as calculated according to Eq. (7), the binding site size was obtained from the plot of $I - I_{\text{DNA}}/I_{\text{DNA}}$ vs. [DNA], Fig. 8 (only shown for Ph_3SnL –DNA at both pH values and at 37 °C, others provided as Fig. S9 in supplementary information).

The binding site size (n) was calculated and found greater than 1 (n > 1) for both compound–DNA complexes, Table 4, the reason being same as discussed in previous section. The values of n obtained at both pH values are consistent with those obtained through fluorescence spectroscopy.

3.5. Compound DNA-binding verification by viscometric analysis

Binding mode of interaction as investigated through spectroscopic and electrochemical techniques could be verified by viscosity measurements (Shahabadi et al., 2011). An increase in the relative viscosity of DNA by gradual addition of various concentrations of the compound is indicative of intercalation binding mode (Shahabadi et al., 2011; Liu et al., 1993). This is further attributed to the lengthening of DNA helix as the size of base pair pockets is increased to accommodate the compound as observed for a classical intercalator, ethidium bromide (Shahabadi et al., 2011).

Upon addition of various concentrations of investigated compounds (LH and Ph_3SnL) on fixed concentration of DNA (10 μM) at both stomach (4.7) and blood (7.4) pH, a gradual rise in the curves was observed when values of the relative specific viscosities for the compounds i.e., $(\eta/\eta_o)^{1/3}$ were plotted vs. [compound]/[DNA], Fig. 9. Where, η_o and η are

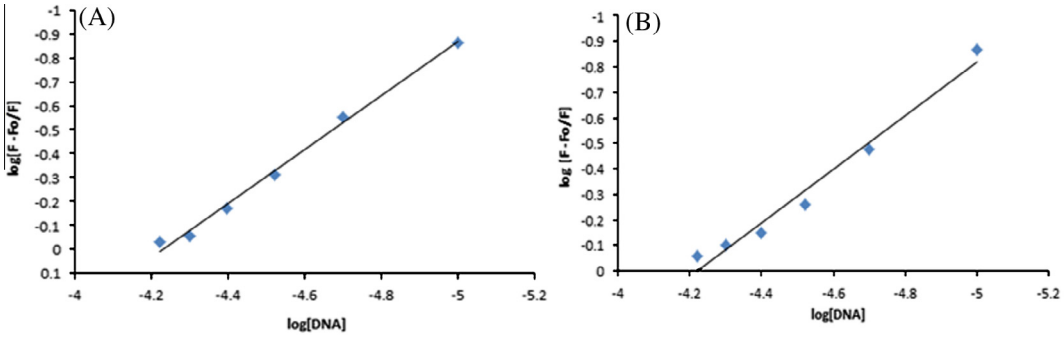

Figure 8 Plots of $I - I_{\text{DNA}}/I_{\text{DNA}}$ vs. [DNA] for determination of binding site size of Ph_3SnL–DNA adducts at pH 4.7 (A) and 7.4 (B) and at 37 °C.

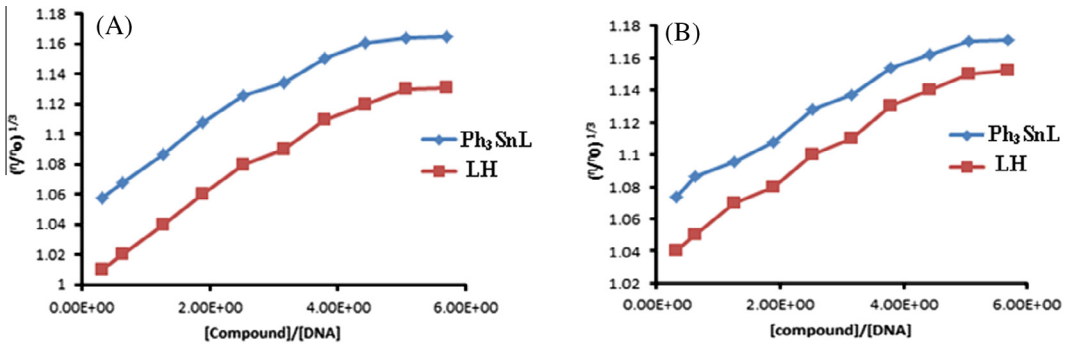

Figure 9 Plots of relative specific viscosity *vs.* [compound]/[DNA] for LH and Ph_3SnL at pH 4.7 (A) and 7.4 (B) and at 37 °C.

the specific viscosity contributions of DNA in the absence and in the presence of the investigated compounds respectively. This behavior could be ascribed as enhancement in the length of DNA helix via intercalation of the compounds within DNA base pairs (Shahabadi et al., 2011; Liu et al., 1993) and further verified our spectroscopic and voltammetric findings.

3.6. Free radical scavenging findings

DPPH assay measures changes in DPPH color from purple to yellow followed by a decrease in absorption at 517 nm after reacting with the test compounds which is indicative of scavenging potential of the antioxidant compound. Both compounds showed no significant DPPH free radical scavenging activity as color changes and decrease in absorption at 517 nm were not observed for various concentrations used. All the compounds have IC_{50} value $>200\ \mu g\ ml^{-1}$.

3.7. Potato disc antitumor findings

The inhibition of *A. tumefaciens*-induced tumors (or Crown Gall) in potato disc tissue is an assay based on antimitotic activity, and can detect a broad range of known and novel antitumor effects (McLaughlin and Rogers, 1998). This assay is based on the hypothesis that antitumor agents might inhibit the initiation and growth of tumors in both plant and animal systems, because certain tumorogenic mechanisms are similar in plants and animals (Coker et al., 2003). The results obtained from potato disc antitumor assay and from other most commonly used antitumor screening assays had shown good correlation as tumor induction mechanisms are reported to be similar in both plants and animals (Rehman et al., 2001). Both compounds (LH and Ph_3SnL) were investigated against *A. tumefaciens* (At 10) for their antitumor potentials. Effect of increasing concentrations of both compounds on tumor formation ability of bacterium was examined and IC_{50} values were calculated. Vincristine (positive control) showed 100% tumor inhibition at all the concentrations tested whereas DMSO (negative control) has no interference with the activity of bacterium to induce tumors. Furthermore, the inhibition was observed in a dose dependent manner with the highest inhibition at $200\ \mu g\ ml^{-1}$ concentration. Antitumor activity can also be determined by 50% inhibitory concentration (calculated by inhibition curves of four concentrations tested for each compound). Among both compounds, Ph_3SnL exhibited the best tumor inhibitory activity with lowest IC_{50} value of $14.02\ \mu g\ ml^{-1}$, Table 5.

4. Conclusion

(*Z*)-4-(4-cyanophenylamino)-4-oxobut-2-enoic acid (LH) and its new triphenyltin(IV) derivative (Ph_3SnL) were synthesized, characterized and investigated for in-vitro binding with DNA as well as bioactivities using spectroscopy (UV–Visible, fluorescence), cyclic voltammetry and bioassays. Spectral and voltammetric responses as well as kinetic and thermodynamic data interpretation (i.e. binding constants, K_b, binding site size, n, and free energy change, ΔG) revealed spontaneous binding of both the compounds with DNA via intercalation. Experimental evidences from both spectroscopic techniques and cyclic voltammetry were comparable and among two compounds Ph_3SnL showed comparatively stronger binding with DNA at both the pH {stomach (4.7) and blood (7.4)} and at 37 °C. In general the binding was evaluated greater at stomach pH. Intercalative binding mode was further verified by viscosity measurements which showed an increasing trend in the relative viscosity of DNA when various concentrations of the compound were added gradually. Antioxidant and antitumor activities through biological assays showed no significant antioxidant activity of both the compounds, while the lowest IC_{50} value was evaluated for Ph_3SnL which showed its best tumor inhibitory activity than that of LH. Results obtained for antitumor potential and DNA binding studies (K_b values) are correlated with each other and further authenticate the significance of our present investigations. These promising results of quantitative findings through both chemical and biological analysis and further investigations in this direction will hopefully lead to find out more effective metal based anticancer drug candidates.

Acknowledgements

This work is supported by the Department of Chemistry, Faculty of Science, Allama Iqbal Open University Islamabad, Pakistan.

Appendix A. Supplementary data

Supplementary data associated with this article can be found, in the online version, at http://dx.doi.org/10.1016/j.arabjc.2014.08.018.

References

Ahmad, M.S., Hussain, M., Hanif, M., Ali, S., Qayyum, M., Mirza, B., 2008. Chem. Biol. Drug. Des. 71, 568.

Alama, A., Tasso, B., Novelli, F., Sparatore, F., 2009. Drug Discov. Today 14, 500.

Ali, S., Shahzadi, S., Bhatti, M.H., 2007. Structural and biological chemistry of organotin(IV) complexes. In: Yamamoto, K. (Ed.), Advances in Organometallic Chemistry Research. Nova Science Publisher, USA, pp. 139–175 (Chapter 6).

Arjmand, F., Jamsheera, A., Afzal, M., Tabassum, S., 2012. Chirality 24, 977.

Arshad, N., Abbas, N., Bhatti, M.H., Rashid, N., Tahir, M.N., Saleem, S., Mirza, B., 2012a. J. Photochem. Photobiol. B: Biol. 117, 228.

Arshad, N., Yunus, U., Razzque, S., Khan, M., Saleem, S., Mirza, B., Rashid, N., 2012b. Eur. J. Med. Chem. 47, 452.

Arshad, N., Farooqi, S.I., Bhatti, M.H., Saleem, S., Mirza, B., 2013. J. Photochem. Photobiol. B: Biol. 125, 70.

Aslanoglu, M., 2006. Anal. Sci. 22, 439.

Aslanoglu, M., Isaac, C.J., Houlton, A., Horrocks, B.R., 2000. Analyst 125, 1791.

Babkina, S.S., Ulakhovich, N.A., 2005. Anal. Chem. 77, 5678.

Bhatti, M.H., Yunus, U., Mussarat, N., Helliwell, M., Prendergast, R., 2013. Acta Cryst. E69, m427.

Camm, K.D., McGowan, P.C., 2009. In: Hadjiliadis, N., Sletten, E. (Eds.), Rhodium and Tin–DNA Interactions and Applications. John Wiley & Sons Ltd, Chichester, UK, pp. 301–315, Chapter 10.

Carter, M.T., Rodriguez, M., Bard, A.J., 1989. J. Am. Chem. Soc. 111, 8901.

Charak, S., Jangir, D.K., Tyagi, G., Mehrotra, R., 2011. J. Mol. Struct. 1000, 150.

Coker, P.S., Radecke, J., Guy, C., Camper, N.D., 2003. Phytomedicine 10, 133.

El-Sherif, A.A., 2012. J. Solution Chem. 41, 1522.

Feng, X.Z., Lin, Z., Yang, L.J., Wang, C., Bai, C.L., 1998. Talanta 47, 1223.

Gielen, M., 1996. Coord. Chem. Rev. 151, 41.

Hadjikakou, S.K., Hahjiliadis, N., 2009. Coord. Chem. Rev. 253, 235.

Hajin, R., Ekhlasi, E., Daneshvar, R., 2012. Eur. J. Chem. 9, 1587.

Ibrahim, M.S., Shehata, I.S., Al-Nateli, A.A., 2002. J. Pharm. Biomed. Anal. 28, 217.

Kaluderovic, G.N., Paschke, R., Prashar, S., Gomez-Ruzi, S., 2010. J. Organomet. Chem. 695, 1183.

Kohn, K.W., Waring, M.J., Glaubiger, D., Friedman, C.A., 1975. Cancer Res. 35, 71.

Kuntz Jr., I.D., Gasparro, F.P., Johnston Jr., M.D., Taylor, R.P., 1968. J. Am. Chem. Soc 90, 4778.

Li, N., Ma, L., Yang, C., Guo, L., Yang, X., 2005. Biophys. Chem. 116, 199.

Liu, F., Meadows, K.A., McMillin, D.R., 1993. J. Am. Chem. Soc. 115, 6699.

McLaughlin, J.L., Rogers, L.L., 1998. Drug Inf. J. 32, 513.

Nagy, L., Pellerito, L., Fiore, T., Nagy, E., Pellerito, C., Szorcsik, A., Scopelliti, M., 2008. Advan. Organomet. Chem. 57, 353.

Nath, M., Pokharia, S., Yadav, R., 2001. Coord. Chem. Rev. 215, 99.

Nawaz, H., Akhter, Z., Yameen, S., Siddiq, H.M., Mirza, B., Rifat, A., 2009. J. Organomet. Chem. 694, 2198.

Niranjana, E., Naik, R.R., Swamy, B.E.K., Bodke, Y.D., Sherigara, B.S., Jayadevappa, H., Badami, B.V., 2008. Int. J. Electrochem. Sci. 3, 980.

Niu, J., Cheng, G., Dong, S., 1994. Electrochim. Acta 39, 2455.

Pettinari, C., Marchetti, F., 2008. Chemical and biotechnological developments in organotin cancer chemotherapy. In: Davies, A.G., Gielen, M., Pannell, K.H., Tiekink, E.R.T. (Eds.), Tin Chemistry: Fundamentals, Frontiers and Applications. John Wiley & Sons, pp. 454–468 (Chapter 4.4).

Randles, J.E.B., 1948. Trans. Faraday Soc. 44, 322.

Rehman, A., Choudhary, M.I., Thomsen, W.J., 2001. Bioassay Techniques for Drug Development. Harwood Academic Publishers, The Netherlands, p. 9.

Rehman, S., Choudhary, M.A., Bhatti, M.H., Ali, S., 2012. J. Iran. Chem. Soc. 9, 35.

Reichmann, M.E., Rice, S.A., Thomas, C.A., Doty, P., 1954. J. Am. Chem. Soc. 76, 3047.

Ruiz, V.G., Olives, A.I., Antonia, M., Martín, M.A., Ribelles, P., Ramos, M.T., Menéndez, J.C., 2011. Biomedical Engineering, Trends, Research and Technologies, Edited by Dr. Sylwia Olsztynska, ISBN 978-953-307-514-3, published in print edition January, pp. 65–90.

Sambrook, J., Fritsch, E.F., Maniatis, T., 1989. Molecular Cloning: A Laboratory Manual. Cold Spring Harbor, New York.

Sevcik, A., 1948. Collect. Czech. Chem. Commun. 13, 349.

Shahabadi, N., Fatahi, A., 2010. J. Mol. Struct. 970, 90.

Shahabadi, N., Kashanian, S., Mahdavi, M., Sourinejad, N., 2011. Bioinorg. Chem. Appl. 2011, 10.

Shujha, S., Shah, A., Zia-ur-Rehman, Ali, N., Muhammad, S., Qureshi, R., Khalid, N., Meetsma, A., 2010. Eur. J. Med. Chem. 45, 2902.

Sirajuddin, M., Ali, S., Mckee, V., Sohail, M., Pasha, H., 2014. Eur. J. Med. Chem. 84, 343.

Tabassum, S., Pettinari, C., 2006. A. J. Organomet. Chem. 691, 1761.

Tabassum, S., Mathur, S., Arjmand, F., Mishra, K., Banerjee, K., 2012. Metallomics 4, 205.

Tiekink, E.R.T., 1991. Appl. Organomet. Chem. 5, 1.

Tiekink, E.R.T., 1994. Trends. Organomet. Chem. 1, 71.

Wang, Q., Wang, X., Yu, Z., Yuan, X., Jiao, K., 2011. Int. J. Electrochem. Sci. 6, 5470.

Xu, Z., Bai, G., Dong, C., 2005. Bioorg. Med. Chem. 13, 5694.

Xu, Z.H., Chen, F.J., Xi, P.X., Liu, X.H., Zeng, Z.Z., 2008. J. Photochem. Photobiol. A: Chem. 196, 77.

Yang, P., Guo, M., 1999. Coord. Chem. Rev. 185–186, 189.